

MASS DIFFUSION IN RESISTIVE HEAD THERMAL PRINTING

I. M. Hodge and D. S. Ross
Eastman Kodak Research Laboratories
Rochester, NY 14650, USA

1. INTRODUCTION

Resistive Head Thermal Printing depends on thermally activated diffusion of dye from a donor to a receiver layer. Because of its fundamental importance, it is desirable to fully understand this diffusion process. In this paper we describe a diffusion model that describes the dye transfer process with remarkable accuracy. Experimentally, the process is known to be influenced by the glass transition temperature, T_g , of the donor and receiver polymers, and plasticization by the dyes. These and other experimental data suggested that dye diffusivities were determined by polymer dynamics, and should therefore scale as $T-T_g$. Because both T and T_g vary with spatial position, and because T_g is a function of concentration, a finite element method was needed to solve the diffusion equations.

2. THE MODEL

The model was one-dimensional and had a single diffusant. Concentration partitioning between the donor and receiver layers could be specified, and each layer was characterized by independent thermal and mass diffusivities.

Heating energy was controlled by pulse count modulation. For the sensitometer for which all experimental and computational data were obtained, up to 64 pulses were applied in groups of eight to produce eight levels of image density. The maximum pulse train of 64 pulses was applied in 32 milliseconds. Traversal of the heater took 64 milliseconds, or twice the pulsing cycle time. Each pulse was followed by three pulsewidths of zero signal to give a 25% duty cycle. Because of this rapid heater pulsing, temperatures at the heater interface undoubtedly fluctuated significantly. This was confirmed by simplified thermal transfer calculations that suggested temperature oscillations of about 20°C at the centers of the heater elements (less near the edges). These were not included in the calculations, because of the need to shorten computation time and because mass diffusion was slow compared with thermal diffusion, so that any temperature fluctuations would be dampened out. The increase in average temperature due to heat buildup during pulsing, suggested by experimental and thermal modeling results, and heat loss and build-up between groups of

pulses, were also neglected. The simplified time-temperature profiles consisted of an instantaneous increase to a temperature that was held constant for the duration of pulsing, with the temperature and hold time increasing with the number of pulses per cycle. Cooling was also assumed to be instantaneous, thus freezing in the computed dye concentration profiles. Temperatures at the donor/receiver interface were estimated from several independent sets of experimental data obtained using a variety of techniques. They are given in Table 1, together with the heater temperatures needed to generate them.

Thermal diffusivities of polymers were fixed at $10^{-3} \text{ cm}^2 \text{ sec}^{-1}$, about four or more orders of magnitude larger than typical mass diffusivities. Thus, if rigorous calculations of temperature gradients and transients had been attempted, almost all the computing time would have been spent on them rather than on the dye concentration profiles that were of central interest. Accordingly, major simplifications were made for the temperature calculations. It was assumed that steady state temperature gradients were established instantly, and that their magnitudes were determined by the heater temperature and the fixed ambient temperature at the bottom of the receiver support (27°C). Temperature gradients were initially estimated using a PC based two-dimensional finite element heat transfer program. For distances less than about 20 microns from the heater, temperature gradients were computed to be about $8^\circ\text{C micron}^{-1}$ at D_{max} and about $2^\circ\text{C micron}^{-1}$ in the toe. At further distances from the heater the gradient diminished, and to reproduce the gradients at the donor-receiver interface in the linear approximation the receiver support was made about ten times thinner than the true value.

The donor sheet was modeled as a 6.5 micron polyester support with varying thicknesses of a dye containing donor layer. The receiver sheet was modelled as a 3 micron receiving layer on a receiver support. The donor and receiving layers were divided into 10 and 100 subintervals, respectively. Donor layer thicknesses were assumed to be an average of those before and after transfer at D_{max} (see below).

Dye mass diffusivities, D , were a function of temperature, T , and concentration, c . The diffusion equations to be solved were of the form

$$\frac{\partial c}{\partial t} = \frac{\partial}{\partial x} \left(D(x) \frac{\partial c}{\partial x} \right) \quad (1a)$$

$$D(x) = D[T(x), c(x)] \quad (1b)$$

The concentration dependence of D was specified in terms of a concentration dependent T_g , so that

$$D(x) = D\{T(x), T_g[c(x)]\} \quad (1c)$$

The WLF equation was used for D as a function of T and T_g :

$$D = A \exp\left(\frac{-B}{T - T_g(c) + C_2}\right) \quad (2)$$

where A, B and C_2 are constants. Experimental data for $T_g(c)$ were well fitted by the empirical expression

$$T_g(c) = T_g^0 \exp[-(k \cdot c)^\beta] \quad 1 \geq \beta > 0 \quad (3)$$

where T_g^0 is the glass temperature of the polymer, c is the weight fraction of dye, and k and β are adjustable constants. This expression gave an excellent description of the rapid decrease in T_g at small dye concentrations.

Equation 2 exhibits a singularity at $T = T_g - C_2$ that was avoided by using an Arrhenius term for temperatures near and below the singularity temperature. The final form for $D(T, T_g)$ was

$$D = A_1 \exp(-E/RT) + A_2 \exp\left(\frac{-B}{T - T_g(c) + C_2}\right) \quad T > T_g(c) - C_2/1.1 \quad (4a)$$

$$= A_1 \exp(-E/RT) \quad T < T_g(c) - C_2/1.1 \quad (4b)$$

A partitioning ratio between donor and receiver polymers, K, was estimated from transfer efficiency and penetration depth data, assuming linear concentration profiles in the donor and receiver after transfer. Preliminary modeling results indicated that the concentration gradient in the receiver was about twice that in the donor. With these assumptions, K is given by

$$K \equiv \frac{c(\text{receiver})}{c(\text{donor})} = \frac{4ldf}{[2d^2 - f(l^2 + 2d^2)]} \quad (5)$$

$$l = \frac{1.16 \times 10^{-4}}{\rho} \left(1 - \frac{x \cdot f}{2}\right) W \quad (6)$$

where l is the donor thickness after transfer, d is the penetration depth, f is the fraction of dye originally in the donor that is transferred, x is the weight fraction of dye in the donor before transfer, W is the donor layer

laydown in gm m^{-2} (dye and polymer, before printing), and ρ is the mass density of the donor+polymer in gm cm^{-3} . The temperature dependence of K was neglected.

In addition to the mathematical simplifications and approximations described above, several physical approximations were also made:

1. Temperatures were assumed to be unaffected by dye diffusion, i.e., heat transfer was decoupled from mass transfer. This was justified by the negligible maximum heats of transfer for the dyes, estimated as the heat of fusion for dye melting.

2. Kinetics of the glass transition were ignored. These were expected to be important only at low densities where temperatures are close to T_g , and in any case are so complex that it would have been impractical to include them.

3. The possible effects of air gaps or other interfacial defects, between either the donor sheet and heater, or donor and receiver, were not explicitly specified. However, their effects were implicit in the assumed heater temperatures and temperature gradients.

4. Thinning of the donor as dye diffused out was neglected. This was compensated for approximately by using donor thicknesses that were an estimated average of the values before and after transfer at D_{max} .

Equation 3 parameters for the concentration dependence of T_g , the WLF constants, and partitioning coefficients, are given in Table 2. Apart from K and T_g^0 , these parameters were kept constant for all dye and receiver combinations. The WLF parameters were constrained to lie within the ranges observed for most polymers, about 500 to 1000 K for B and 40 to 100 K for C_2 . The pre-exponential factors determine the absolute diffusivities D , and were estimated using the one-dimensional Einstein relation:

$$D = d^2/(2t) \quad (7)$$

where d is the penetration depth and t is the printing time. For the observed penetration depth into bisphenol A polycarbonate (BPAPC) of about 1.6 micron at D_{max} , and a printing time of 64 msec per pixel, diffusivities were estimated to be about $5 \times 10^{-8} \text{ cm}^2 \text{ sec}^{-1}$ for D_{max} . Further constraints were imposed by experimental Forced Raleigh Scattering (FRS) data for photoactive dyes in the donor and receiver polymers. The data of Sillescu and coworkers⁽¹⁾ were used for the polycarbonate receiver, and FRS data obtained by Hodge, Lander, and Wesson⁽²⁾ were used for the donor. The preliminary WLF parameters were then adjusted to give the best fit to experimental data on transfer efficiency and penetration depths for transfer of cyan dye into BPAPC. The

activation energy, E , chosen for eqs. (4) was sufficiently small to ensure that the Arrhenius term never exceeded the WLF term at high temperatures. The pre-exponential factor A_1 was determined by equating the Arrhenius and WLF terms at $T=T_g^0$.

A finite element code was developed to solve the nonlinear diffusion equations. This was written in Fortran using double precision variables throughout.

3. RESULTS

We first demonstrate that the selected parameters are physically reasonable. The limiting zero concentration dye diffusivities calculated using the parameters given in Table 2 are compared with experimental data in Figure 1. Figure 1A shows the WLF prediction and experimental FRS diffusivity data for methyl yellow in the cellulose ester donor ($T_g^0=140^\circ\text{C}$). Figure 1B shows the WLF prediction and experimental data for a dye in BPAPC obtained by Sillescu and coworkers using FRS(1), and unpublished data for the magenta dye used throughout this work(3). The WLF predictions for BPAPC are shown for $T_g=150^\circ\text{C}$, about 10°C lower than that of the pure polymer, to allow for dye plasticization in the Sillescu data and a small amount of plasticization by the silicone oil used in the magenta dye diffusion experiments. The agreement for the donor is excellent and that for the receiver is acceptable.

Calculated transfer efficiencies for cyan diffusion from the donor ($T_g^0=142^\circ\text{C}$) into BPAPC receiver ($T_g^0=160^\circ\text{C}$) are compared with experimental data in Figure 2, where transfer efficiencies are expressed as the percentage of total available dye in the donor that is transferred. Agreement is within experimental uncertainty. The predictive accuracy of the model is further demonstrated by comparing experimental and calculated transfers into a lower T_g BPAPC receiver containing a tetra-alkoxy benzene plasticizer to bring its T_g^0 down to 90°C . The calculated results for cyan are compared with experimental data in Figure 3, and agreement is again within experimental uncertainty. This agreement may be fortuitously good, however, because the single diffusant model could not take into account probable diffusion of the plasticizer back into the donor.

Different dyes were modeled by changes in the partitioning ratios K (Table 2). A particularly severe test of the model is the prediction of transfer efficiencies for magenta and yellow dyes into plasticized PC receiver, since this involves changes in both receiver T_g^0 and partitioning ratio K . The results are compared with experimental data in Figures 4 and 5 for the magenta and yellow dyes, respectively. Agreement is good.

Modeling calculations of the effects on transfer efficiency of energy input, donor thickness, and dye concentration in the donor, were made using the cyan value for K (Table 2). The thicknesses associated with total (dye+polymer) donor laydowns of 40, 70, and 100 mg ft⁻² were 0.35, 0.60, and 0.86 microns, respectively. As noted above, these thicknesses were less than those calculated from the original donor laydowns (assuming a mass density of 1.1 gm cm⁻³), to compensate for the neglect of donor thinning during dye transfer. The results for cyan diffusion into BPAPC receiver are summarized in Table 3. Agreement is very good, within experimental uncertainty in most cases. The tendency for the calculated efficiencies at D_{\max} to be too high is probably due to a greater fractional change in donor thinning at the highest transfer efficiencies.

DISCUSSION

It is apparent from the data given here that the model gives a good to excellent account of mass transfer as a function of energy input, initial dye concentration in the donor, donor thickness, and receiver T_g . It is concluded that the essential features of mass transfer in Resistive Head Thermal Printing are contained in the model. This success indicates that mass transfer does indeed occur by diffusion of dye from the donor to the receiver, and that it is controlled to a large extent by physical factors that determine the mass diffusivities, such as temperature and receiver T_g , and geometric factors such as donor thickness. One aspect of the process where specific molecular interactions are a factor is favorable partitioning of the dye toward the receiver.

REFERENCES

1. J. Coutandin, D. Ehlich, H. Sillescu, and C.-H. Wang, *Macromolecules* **18**, 589 (1985).
2. I. M. Hodge, C. W. Lander, and J. Wesson, unpublished data.
3. G. Byers, unpublished data.

TABLE 1
TEMPERATURES

Pulse Count	Heater (°C)	Donor/Receiver Interface (°C)
64	307	257
56	247	208
48	212	179
40	167	141
32	147	125
24	132	112
16	117	100
8	107	92

TABLE 2
MODEL PARAMETERS

Parameter	Receiver	Donor
Eq. 3		
k	1.24	0.752
β	0.70	0.69
T_g°	90 or 160°C	142°C
Eq 4		
A1 (cm ² sec ⁻¹)	4.00*10 ⁻¹⁰	4.00*10 ⁻¹⁰
E (kcal mole ⁻¹)	5	5
A2 (cm ² sec ⁻¹)	1.30*10 ⁻⁶	1.03*10 ⁻⁶
B (K)	543.9	689.0
C2 (K)	43	100
Eq. 6		
K	0.8 (yellow)	
	1.8 (cyan)	
	3.1 (magenta)	

TABLE 3
CYAN DIFFUSION INTO BPAPC

Donor ^a Thickness	Dye fraction in Donor	Pulses	Penetration Depth ^a	% Transferred obs	calc
<hr style="border-top: 1px dashed black;"/>					
0.35	0.60	64	1.69	86	83
		48	0.51	65	59
		32	0.10	18	23
	0.40	64	1.51	90	82
		48	0.41	55	54
		32	-	-	-
	0.20	64	1.24	84	80
		48	0.30	41	44
		32	0.04	10	9
<hr style="border-top: 1px dashed black;"/>					
0.60	0.60	64	1.71	69	70
		48	0.50	43	39
		32	0.12	12	13
	0.40	64	1.56	68	68
		48	0.41	33	34
		32	0.07	8	9
	0.20	64	1.29	63	65
		48	0.29	25	27
		32	0.04	5	5
<hr style="border-top: 1px dashed black;"/>					
0.86	0.60	64	1.71	59	56
		48	0.49	29	27
		32	0.12	8	9
	0.40	64	0.54	58	46
		48	0.39	24	23
		32	0.07	6	6
	0.20	64	1.26	48	50
		48	0.27	15	18
		32	0.04	5	3

=====
 (a) in microns
 =====

FIGURE 1A
DONOR DIFFUSIVITIES

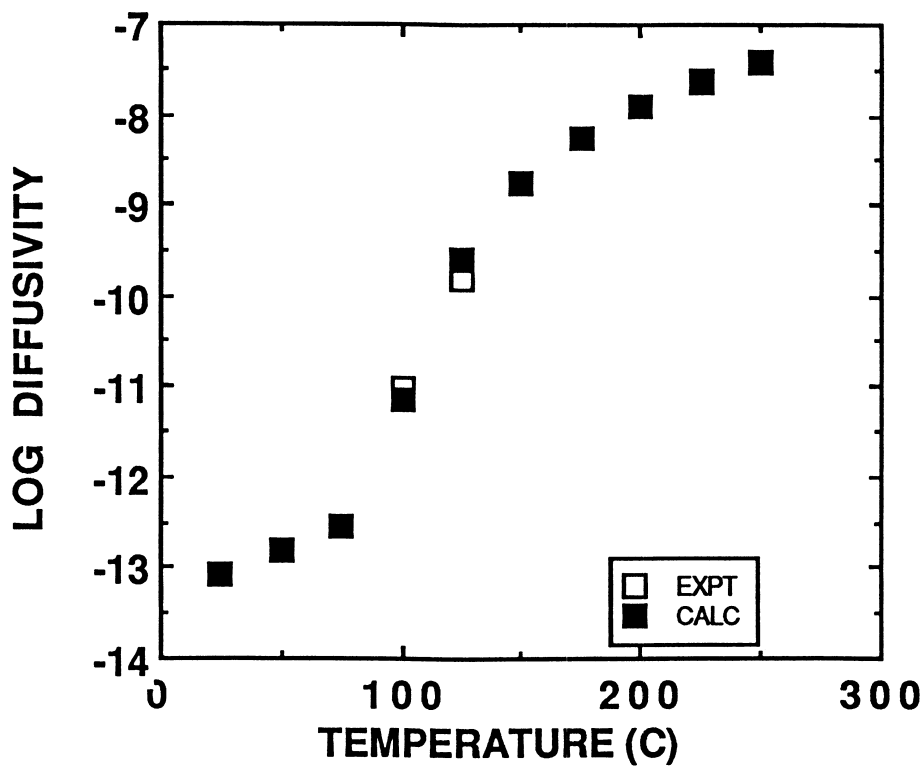


FIGURE 1B
DIFFUSIVITIES IN BPAPC

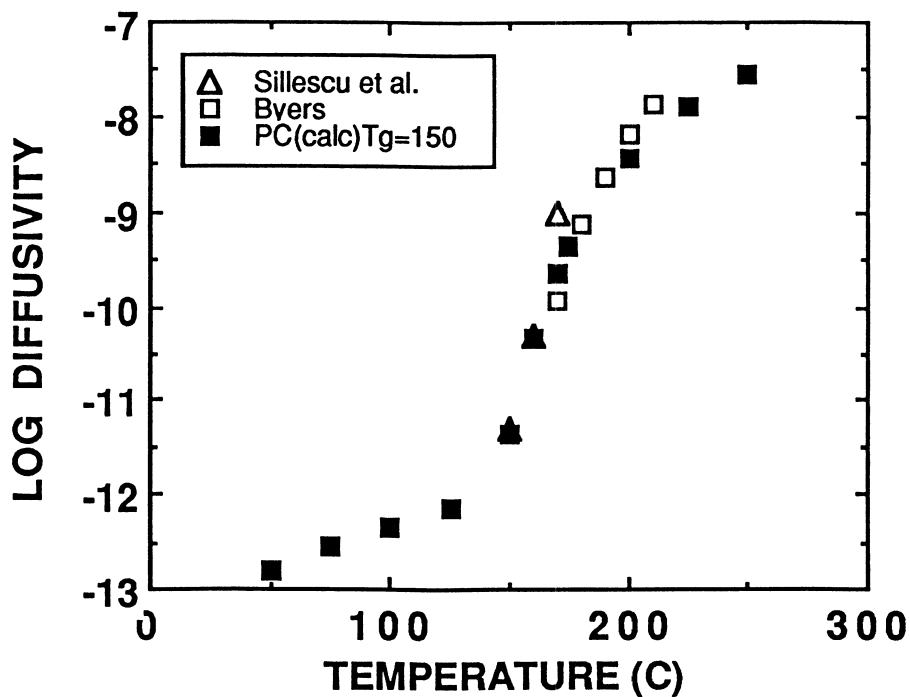


FIGURE 2
CYAN INTO BPAPC

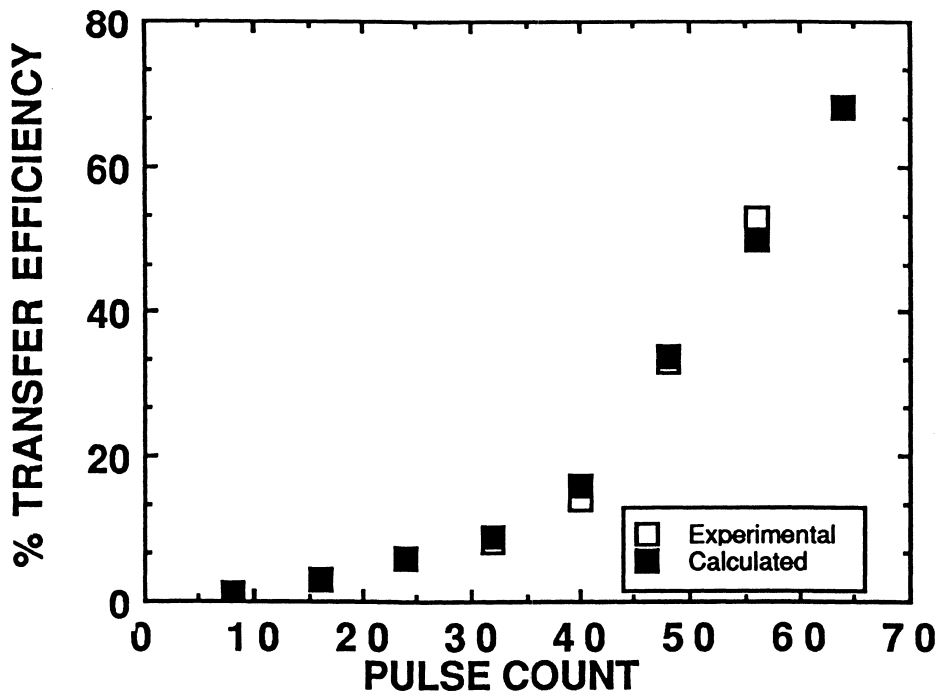


FIGURE 3
CYAN INTO PLASTICIZED BPAPC

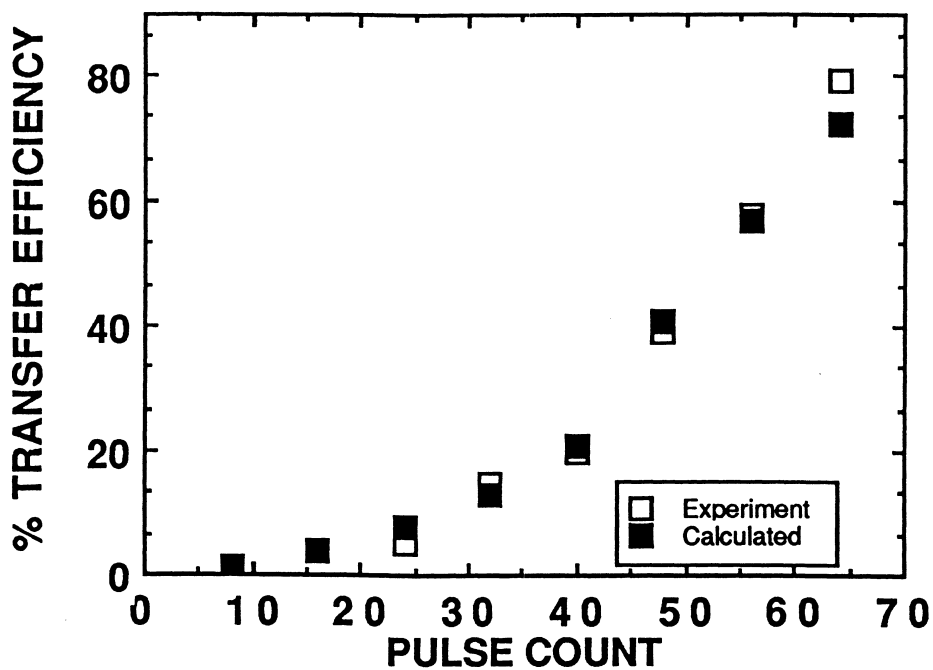


FIGURE 4
MAGENTA INTO PLASTICIZED BPAPC

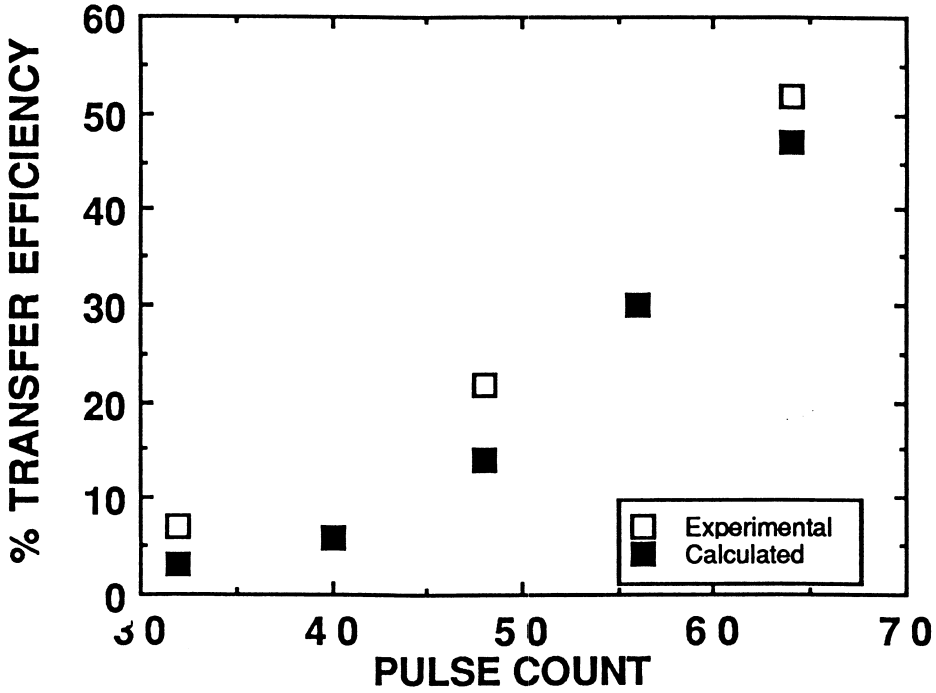


FIGURE 5
YELLOW INTO PLASTICIZED BPAPC

